

The rapidly oscillating Ap star HD 99563 and its distorted dipole pulsation mode

G. Handler,^{1,2} W. W. Weiss,¹ R. R. Shobbrook,³ E. Paunzen,¹ A. Hempel,⁴
S. K. Anguma,⁵ P. C. Kalebwe,⁶ D. Kilkeny,² P. Martinez,² M. B. Moalusi,⁷
R. Garrido,⁸ R. Medupe²

¹ *Institut für Astronomie, Universität Wien, Türkenschanzstraße 17, A-1180 Wien, Austria*

² *South African Astronomical Observatory, P.O. Box 9, Observatory 7935, South Africa*

³ *Research School of Astronomy and Astrophysics, Australian National University, Canberra, ACT, Australia*

⁴ *Observatoire de Genève, Chemin des Maillettes 51, CH-1290 Sauverny, Switzerland*

⁵ *Department of Physics, Mbarara University of Science and Technology, P. O. Box 1410, Mbarara, Uganda*

⁶ *Physics Department, The University of Zambia, P. O. Box 32379, Lusaka, Zambia*

⁷ *Department of Physics, University of the North-West, Private Bag X2046, Mmabatho 2735, South Africa*

⁸ *Instituto de Astrofisica de Andalucia, Apt. 3044, E-18080 Granada, Spain*

Accepted 2005 nnnn nn. Received 2005 nnnn nn; in original form 2005 nnnn nn

ABSTRACT

We undertook a time-series photometric multi-site campaign for the rapidly oscillating Ap star HD 99563 and also acquired mean light observations over two seasons. The pulsations of the star, that show flatter light maxima than minima, can be described with a frequency quintuplet centred on $1557.653 \mu\text{Hz}$ and some first harmonics of these. The amplitude of the pulsation is modulated with the rotation period of the star that we determine with 2.91179 ± 0.00007 d from the analysis of the stellar pulsation spectrum and of the mean light data. We break the distorted oscillation mode up into its pure spherical harmonic components and find it is dominated by the $\ell = 1$ pulsation, and also has a notable $\ell = 3$ contribution, with weak $\ell = 0$ and 2 components. The geometrical configuration of the star allows one to see both pulsation poles for about the same amount of time; HD 99563 is only the fourth roAp star for which both pulsation poles are seen and only the third where the distortion of the pulsation modes was modelled. We point out that HD 99563 is very similar to the well-studied roAp star HR 3831. Finally, we note that the visual companion of HD 99563 is located in the δ Scuti instability strip and may thus show pulsation. We show that if the companion was physical, the roAp star would be a $2.03 M_{\odot}$ object, seen at a rotational inclination of 44° , which then predicts a magnetic obliquity $\beta = 86.4^{\circ}$.

Key words: stars: variables: other – stars: oscillations – techniques: photometric – stars: individual: HD 99563 – stars: individual: XY Cr

1 INTRODUCTION

Where the lower part of the classical instability strip intersects the main sequence, three distinct classes of multiperiodically pulsating variables can be found. The γ Doradus stars pulsate in gravity modes of high radial order and have periods of the order of one day (Kaye et al. 1999). The δ Scuti stars have periods of the order of a few hours (Breger 1979) and are thus pressure and gravity mode pulsators of low radial order.

The fastest pulsations in this domain in the HR diagram

are however excited in the rapidly oscillating Ap (roAp) stars (Kurtz 1982, Kurtz & Martinez 2000), with typical periods around 10 minutes, indicating pressure modes of high radial overtones. The photometric semi-amplitudes associated with these pulsations are in most cases only a few mmag, which makes them difficult to detect. The roAp stars are also remarkable due to their spectral peculiarities, since they are pulsating representatives of cool magnetic Ap stars of the SrCrEu subtype.

The magnetic fields of Ap stars cause elemental segre-

gation on the stellar surface. In other words, the chemical elements are arranged in patches on the stellar surface (see, e.g., Kochukhov et al. 2004 or Lueftinger et al. 2003 for well-documented examples). This causes modulation of the mean apparent brightness of the star with the rotation period. As the chemical elements show some alignment with the magnetic poles, the rotational light curves show a single-wave structure if only one magnetic pole is seen and a double-wave variation if both magnetic poles come into view during a rotation cycle.

The strong magnetic fields present in the roAp stars are usually not aligned with the stellar rotation axis. Since the pulsation axis does however coincide with the magnetic axis, the roAp stars are oblique pulsators (Kurtz 1982). This means that the pulsation modes excited in the roAp stars are seen at different aspects during the rotation cycle, which, for nonradial modes, causes amplitude modulation over the rotation period (which can then be inferred) and allows us to put constraints on the geometry of the pulsator.

The oblique pulsator model (OPM), in its simplest form, then predicts that (except for special geometric orientations of the axes) dipole ($\ell = 1$) pulsation modes will be split into equally spaced triplets. Quadrupole ($\ell = 2$) modes will give rise to equally spaced frequency quintuplets, where the spacing of consecutive multiplet components is exactly the stellar rotational frequency.

The magnetic field of the roAp stars affects the pulsations in two additional ways. Firstly, the pulsation frequencies are shifted with respect to their unperturbed value (Cunha & Gough 2000) and secondly, the pulsation modes are distorted so that a single spherical harmonic can no longer describe them fully (e.g., Kurtz, Kanaan & Martinez 1993, Takata & Shibahashi 1995). This is observationally manifested by the presence of additional multiplet components surrounding the first-order singlets, triplets or quintuplets, which are spaced by integer multiples of the rotation frequency.

For a long time, the predominant observing method for studying the pulsations of roAp stars was time-resolved high-speed photometry, yielding interesting results on the pulsational behaviour, geometry and asteroseismology of these stars (e.g., see Matthews, Kurtz & Martinez 1999). The most recent observational advances however came from time-resolved spectroscopy: since the vertical wavelengths of the pulsation modes are comparable to the size of the line-forming regions in the atmospheres of these stars, the vertical structure of the atmospheres can be resolved (Ryabchikova et al. 2002, Kurtz, Elkin & Mathys 2003).

Spectroscopy is also more sensitive to the detection of roAp star pulsations than photometry. Due to the vertical stratification of chemical elements in their atmospheres (e.g. Ryabchikova et al. 2002) the pulsational radial velocity amplitudes of some spectral lines (most notably rare earth elements) can reach several kilometres per second.

The most extreme example of such high radial velocity amplitudes is HD 99563 (XY Crt). This star was photometrically discovered to pulsate by Dorokhova & Dorokhov (1998) and was confirmed by Handler & Paunzen (1999). Elkin, Kurtz & Mathys (2005) discovered pulsational radial velocity variations with semi-amplitudes of up to 5 km s^{-1} for some EuII and TmII lines in their time-resolved spectroscopy of this star. Such high amplitudes are capable of yielding in-

formation on the structure of the atmospheres of Ap stars with the best possible signal to noise.

However, one important piece of information that spectroscopy cannot supply at this point is detailed knowledge of the stellar pulsation spectrum. The reason is that the largest telescopes are necessary for obtaining spectra of the required time resolution and signal to noise. However, observing time on these telescopes is sparse. Therefore, lengthy photometric measurements of these stars on small telescopes are still required to decipher the pulsational spectra fully.

To this end, we included HD 99563 as a secondary target in a multi-site campaign originally devoted to the roAp star HD 122970 (Handler et al. 2002) to be observed at times when the latter star was not yet accessible. However, HD 99563 turned out to be quite interesting, which is why we continued to observe it after the original campaign was finished. We also acquired some mean-light observations of HD 99563 in an attempt to determine its rotation period. In this paper, we report the results of these measurements.

2 OBSERVATIONS AND REDUCTIONS

2.1 The high-speed photometry

Our multi-site time-series photometric observations were obtained with seven different telescopes at four observatories: the 0.75m T6 Automatic Photometric Telescope at Fairborn Observatory (FAPT) in Arizona, the 0.5m, 0.75m, 1.0m and 1.9m telescopes at the South African Astronomical Observatory (SAAO), the 0.6m reflector at Siding Spring Observatory (SSO) in Australia and the 0.9m telescope at Observatorio de Sierra Nevada (OSN) in Spain. Whereas the latter observations consisted of Strömgren *uvby* photometry, the other telescopes used the B filter only. The measurements are summarised in Table 1.

The time-series photometry was generally acquired as continuous 10-second integrations. Large apertures (> 35 arcseconds) were employed to minimise the contributions of seeing and guiding. The observations of the target star were interrupted at irregular intervals (depending on the brightness and position of the Moon) to obtain measurements of sky background.

Reductions were performed by first correcting for coincidence losses (dead time correction), then for sky background and extinction. Some low-frequency filtering to remove residual transparency variations or tube sensitivity drifts with time scales longer than 30 minutes was applied by fitting low-order polynomials to the data and by subtracting these. Finally the measurements were binned into 40-second integrations, the times of the observation were converted to Heliocentric Julian Date (HJD) and all the data were joined into a combined single light curve.

Some of our nightly measurements are shown in Fig. 1, clearly containing some interesting features. Firstly, the pulsation amplitude can vary rather dramatically from almost zero to more than 10 mmag peak-to-peak, and it can also be seen to vary during a single night. Secondly, the shape of the light curves near maximum amplitude is peculiar, with the light maxima being flatter than the light minima.

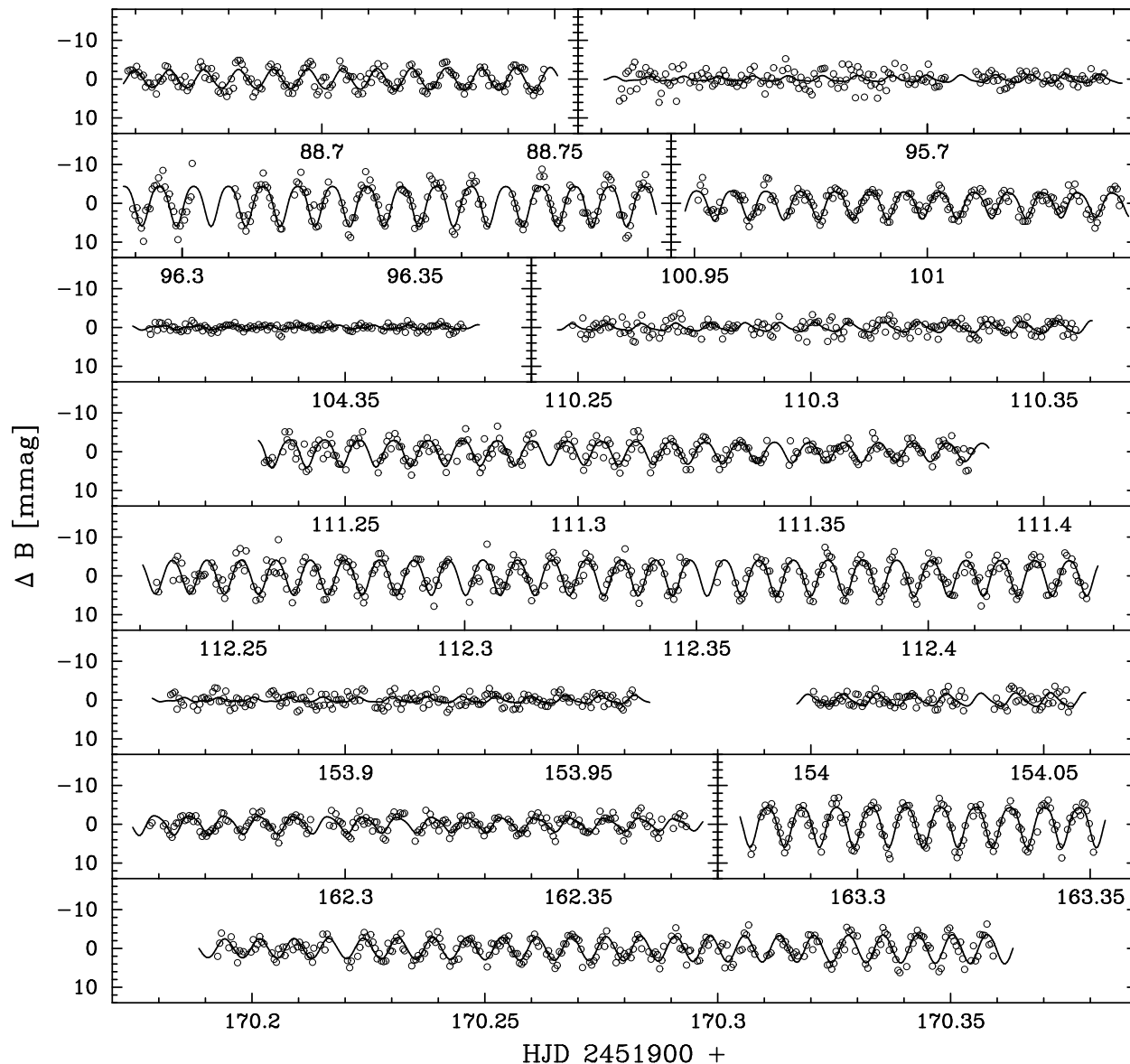


Figure 1. Some light curves of HD 99563 from our multi-site observations showing its diverse nightly behaviour. The solid lines represent the multifrequency fit to be listed in Table 2, to guide the eye.

2.2 The mean light observations

Differential multicolour photometry of HD 99563 was obtained with the 0.75m Automatic Photometric Telescope at SAAO (Martinez et al. 2002) from March 2001 until June 2004. Single-channel differential measurements with respect to the single comparison star HD 99506, which is not known to be variable, in the Johnson-Cousins UBVRI filters were acquired. Again, large apertures ($> 35''$) were used to eliminate effects of scintillation and seeing.

Two nightly UBVRI measurements of HD 99563 were usually taken in between two measurements of HD 99506, ensuring that variations in sky transparency can be readily compensated for, but also aiming at averaging out the effects of the rapid oscillations on the mean magnitude. As the two integrations on the target were separated by about 380 s,

about half the oscillation period, the pulsational signal was strongly suppressed.

The data of both stars were reduced by correction for coincidence losses, sky background and extinction, and the timings were heliocentrically corrected. Differential magnitudes between the variable and the comparison star were computed by simple linear interpolation. After rejection of outliers and merging of the two nightly measurements, a total of 150 differential UBVRI magnitudes of HD 99563 were available.

3 FREQUENCY ANALYSIS (I)

3.1 The high-speed photometry

The reduced B filter light curves were analysed with the computer programme `Period98` using single-frequency

Table 1. Journal of the observations of HD 99563; N_{40} is the number of 40-second data bins obtained in the respective night and σ is the rms scatter of the residual light curves after prewhitening and low-frequency filtering; the remaining columns are self-explanatory.

Telescope	Date (UT)	Start (UT)	Length (hr)	N_{40}	σ (mmag)
FAPT 0.75m	18/03	04:54:24	0.64	55	1.98
FAPT 0.75m	19/03	03:43:40	1.75	140	1.71
FAPT 0.75m	20/03	03:39:41	2.15	180	1.40
FAPT 0.75m	23/03	03:23:03	2.54	208	1.74
FAPT 0.75m	24/03	03:16:41	2.53	210	2.21
FAPT 0.75m	25/03	04:20:58	1.43	119	1.51
FAPT 0.75m	26/03	03:10:24	2.52	209	1.73
FAPT 0.75m	27/03	03:04:34	2.52	200	1.88
SAAO 0.5m	27/03	18:47:49	2.68	188	1.75
SSO 0.6m	28/03	09:49:16	2.01	166	2.04
SAAO 0.5m	28/03	17:59:55	3.36	252	2.14
FAPT 0.75m	29/03	02:58:32	2.52	174	2.14
SSO 0.6m	29/03	09:20:27	3.59	271	2.21
SAAO 0.5m	29/03	17:56:30	3.35	255	1.87
SAAO 0.5m	30/03	20:31:12	0.72	59	1.85
FAPT 0.75m	31/03	02:47:47	2.52	210	2.24
SSO 0.6m	31/03	09:43:39	2.82	235	1.62
SSO 0.6m	01/04	10:41:08	2.18	177	1.48
SAAO 0.5m	02/04	18:03:43	2.96	192	2.19
SAAO 1.0m	03/04	19:34:44	1.29	104	0.59
SSO 0.6m	04/04	09:18:16	2.01	146	1.80
SAAO 1.0m	04/04	19:15:49	1.62	137	0.65
SSO 0.6m	05/04	11:01:34	1.37	101	1.61
FAPT 0.75m	09/04	02:50:41	1.61	131	2.15
SAAO 0.5m	09/04	17:43:48	1.08	64	2.11
SAAO 1.0m	09/04	18:00:40	1.14	98	1.23
OSN 0.9m	09/04	19:54:16	1.61	135	8.2/2.8/3.0/3.7
SAAO 0.5m	10/04	17:50:42	2.59	191	
SAAO 0.5m	11/04	17:27:29	3.64	264	1.62
OSN 0.9m	11/04	20:19:34	4.44	309	7.5/4.4/4.0/4.5
FAPT 0.75m	12/04	02:55:06	1.57	127	
SAAO 0.5m	12/04	17:28:47	6.85	465	1.79
FAPT 0.75m	13/04	02:53:47	1.61	135	1.56
FAPT 0.75m	14/04	03:44:02	0.69	57	2.90
SAAO 0.5m	14/04	17:09:07	4.13	305	1.87
FAPT 0.75m	15/04	02:44:55	1.42	120	1.65
FAPT 0.75m	16/04	02:57:02	1.23	102	1.60
FAPT 0.75m	18/04	02:52:32	0.90	76	1.62
SSO 0.6m	23/04	13:42:01	0.72	54	2.11
SSO 0.6m	27/04	09:01:18	5.04	398	1.71
SAAO 1.9m	30/04	17:14:35	0.69	60	0.95
SAAO 0.75m	15/05	17:11:06	1.61	137	1.57
SSO 0.6m	16/05	11:59:23	0.24	23	2.03
SAAO 0.75m	16/05	20:50:28	0.68	58	1.24
SAAO 0.75m	17/05	18:28:06	1.80	155	1.50
SAAO 0.75m	18/05	16:59:33	3.40	257	1.43
SAAO 0.75m	21/05	19:09:55	2.34	206	1.50
SSO 0.6m	22/05	12:09:16	1.10	94	1.90
SSO 0.6m	24/05	08:38:42	3.72	298	1.41
SSO 0.6m	30/05	08:20:08	1.68	139	1.12
SAAO 0.5m	01/06	18:09:26	2.76	222	1.20
SAAO 0.5m	02/06	18:37:05	1.76	143	1.26
SAAO 0.5m	04/06	17:14:49	3.18	253	1.60
SAAO 0.5m	06/06	19:58:06	0.79	59	2.34
SAAO 0.5m	07/06	16:38:51	2.54	183	1.73
SAAO 0.5m	08/06	16:41:45	3.97	286	2.78
SAAO 0.5m	09/06	16:36:15	4.00	296	1.59
SAAO 0.5m	10/06	18:23:46	1.18	82	1.32
SAAO 0.5m	11/06	17:40:49	2.75	202	1.56
Total	<i>B</i>		125.49	9728	1.82
	<i>uvby</i>		6.05	444	7.7/3.9/3.7/4.3

Fourier and multiple-frequency least-squares techniques (Sperl 1998). This programme has, amongst others, the capabilities of calculating Fourier periodograms, calculating the best fit to the data with all given frequencies simultaneously by minimising the residuals between light curve and fit. Within the multifrequency fitting, combination frequencies (that are in our case expected due to the shape of the light curves) can be fixed to their expected values and their amplitudes and phases can be optimised together with the other independent parameters.

We show the amplitude spectrum of the combined light curve in the uppermost panel of Fig. 2. Two main regions of power are visible, one centered around 1500 μHz and a weaker one around 3100 μHz . The first of the sequence of panels on the left-hand side of Fig. 2 shows the spectral window of the data at an extended scale, computed as the Fourier transform of a single noise free sinusoid with a frequency of 1553.67 μHz and an amplitude of 2.7 mmag. We see some alias patterns about 34.7 μHz away from the central peak. This is the 3 cd^{-1} alias, which is most prominent in our data because of the longitude distribution of the observatories used combined with the short duration of most of the runs. Fortunately, neither this alias, nor any other, will have any influence on our results.

The second panel on the left-hand side contains the amplitude spectrum of the data. It is clearly more complicated than the spectral window. Prewhitening the strongest signal from the data we end up with the residual amplitude spectrum in the third (middle) panel of Fig. 2, left-hand side. Further prewhitening of the strongest signal there reveals another one, and continuing this procedure results in the detection of a fourth frequency in this domain, where no more signals can now be detected.

We continue the frequency analysis in the region around 3100 μHz , showing it in the sequence of panels on the right-hand side of Fig. 2. Following the same strategy as before, we detect five signals in this frequency domain. After prewhitening these, we arrive at the residual amplitude spectrum in the lowest panel of Fig. 2. The noise level at frequencies below $\sim 800\mu\text{Hz}$ is artificially decreased due to our low-frequency filtering.

Consequently, we have separately analysed our longest ($\Delta T > 2$ hr) light curves from the best nights, leaving them unfiltered for low frequencies, and searched them for periodicities. We found no such variations, with detection thresholds of 1.8 mmag for frequencies below 200 μHz , 0.8 mmag for frequencies between 200 and 450 μHz , and 0.5 mmag for frequencies between 450 and 1000 μHz , respectively.

More interesting is the excess mound of amplitude at frequencies around 1500 μHz on top of the essentially monotonically decreasing noise that can be discerned in the lowest panel of Fig. 2. This is the region where four signals have already been detected. The excess mound of amplitude may indicated the presence of further signals or of amplitude/frequency variability of some of the periodicities detected previously. In any case, a preliminary frequency solution derived in this way is listed in Table 2.

We have only accepted signals that satisfy the statistical criterion of $S/N > 4$ for independent oscillations and $S/N > 3.5$ for combination frequencies. These variations are regarded as statistically significantly detected. We refer to Breger et al. (1999) for a more in-depth discussion of this

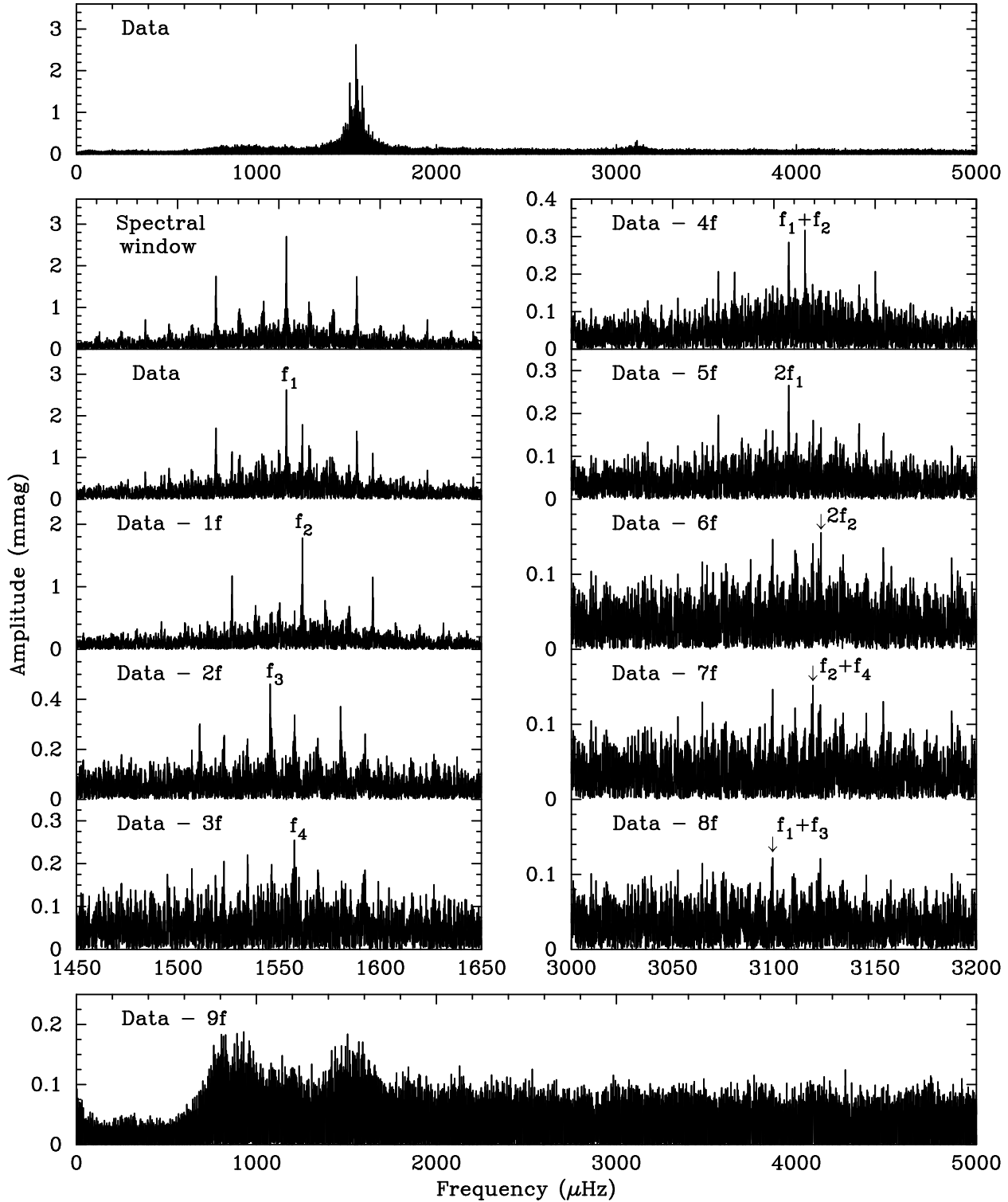


Figure 2. Amplitude spectra of HD 99563 from our multi-site observations with successive prewhitening of the detected frequencies.

criterion, that has turned out to be extremely reliable in the past.

The independent frequencies in Table 2 can, at first sight, not be unambiguously be interpreted within the OPM. Although f_3, f_1 and f_2 form a triplet with a spacing of about 7.95 μHz , f_1, f_4 and f_2 can also be reconciled with a triplet

with a spacing of approximately 3.98 μHz , allowing for a $\sim 3\sigma$ shift in frequency f_4 . In this context it is important to note that the formal error estimates we use here are believed to underestimate the real errors by about a factor of 2 (Handler et al. 2000, Jerzykiewicz et al. 2005), and therefore we cannot simply reject the latter interpretation. Consequently,

Table 2. Preliminary multifrequency solution for our B filter data of the roAp star HD 99563, with the frequencies around 1500 μHz left as free parameters. Error estimates correspond to 1σ values are determined following Montgomery & O’Donoghue (1999).

ID	Frequency (μHz)	B Ampl. (mmag)	S/N
f_1	1553.6780 ± 0.0007	2.69 ± 0.03	49.1
f_2	1561.6286 ± 0.0011	1.80 ± 0.03	32.9
f_3	1545.736 ± 0.004	0.46 ± 0.03	8.4
f_4	1557.639 ± 0.007	0.28 ± 0.03	5.1
$f_1 + f_2$ or $2f_4$	3115.3065	0.32 ± 0.03	9.1
$2f_1$	3107.3559	0.25 ± 0.03	7.2
$2f_2$	3123.2571	0.16 ± 0.03	4.7
$f_2 + f_4$	3119.268	0.14 ± 0.03	3.9
$f_1 + f_3$	3099.414	0.13 ± 0.03	3.6

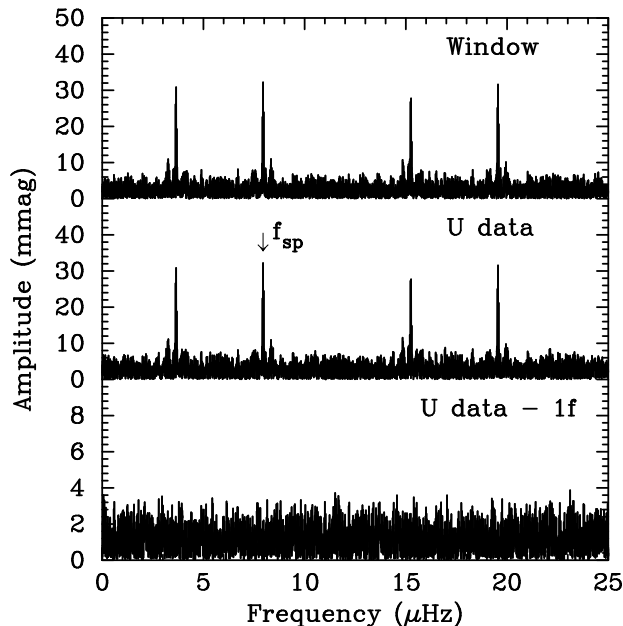


Figure 3. Amplitude spectra of the mean light observations of HD 99563 in the U filter. Upper panel: spectral window function of the time series. Middle panel: amplitude spectrum of the data themselves. Lower panel: residual amplitude spectrum after prewhitening the strongest signal from the data. Note the five times larger ordinate scale of the lower panel.

all four frequencies could even be part of an equally spaced quintuplet with a component missing near 1549.7 μHz .

3.2 The mean light observations

We again used *Period98* for the frequency analysis. Amplitude spectra of the measurements in the five UBVR filters were computed. Although the nominal Nyquist frequency of our observations is 0.5 cd^{-1} ($\sim 6 \mu\text{Hz}$), we carefully examined a frequency range up to 25 μHz . We found variability in all the five passbands, with those in U having the highest amplitude, as shown in Fig. 3.

The upper panel of this graph contains the spectral window function of the data, calculated as the amplitude spectrum of a single noise-free sinusoid with a frequency of

Table 3. The amplitudes and phases of the mean light variations of HD 99563, once more with error estimates from Montgomery & O’Donoghue (1999). The phases are with respect to pulsation amplitude maximum at HJD 2452031.29627.

Filter	Amplitude (mmag)	Phase (rad)
U	31.3 ± 1.0	-0.06 ± 0.03
B	20.4 ± 0.9	-0.00 ± 0.04
V	4.6 ± 0.8	$+3.09 \pm 0.17$
R	9.2 ± 0.8	$+3.09 \pm 0.09$
I	7.3 ± 0.7	$+3.11 \pm 0.10$

7.95 μHz and an amplitude of 31 mmag. There is strong 1 cd^{-1} aliasing (the peak near 20 μHz), and also reflection of the aliasing pattern at frequency zero (peaks near 4 and 15 μHz). Nevertheless, the input signal produces the tallest peak in the window function. This is why we can be sure that the peak labelled in the amplitude spectrum of the data (middle panel of Fig. 3) is also the correct frequency present in the measurements, which is confirmed by the prewhitened amplitude spectrum in the lower panel of this figure that contains noise only.

We encountered the same situation in the B filter data, where the mean light variations also have considerable amplitude. In *VRI* the situation is more complex, as the S/N of the variability is lower. Significant peaks at the same frequencies are however still present, but due to the effects of noise the tallest maxima are found at alias frequencies in *V* and *R*. After prewhitening the signal near 7.95 μHz , the residual amplitude spectra in all filters contain noise only; in particular, no evidence for harmonics or subharmonics of this frequency can be detected.

Consequently, we can describe the variability present in the mean light variations of HD 99563 with a single frequency of $7.9498 \pm 0.0002 \mu\text{Hz}$, as determined from a non-linear least-squares fit to the U data, which have the best signal-to-noise. This frequency is consistent with one of the possible multiplet spacings within the pulsational signals as determined in the previous section, but the ambiguity of whether this frequency or half of it corresponds to the rotation period of HD 99563 is not yet resolved. The amplitudes and phases of the mean light variations with respect to the frequency of 7.9498 μHz are listed in Table 3.

This table shows that the mean light maxima in the U and B filters occur at the same time as pulsation amplitude maximum in the light curves. In the V, R and I filters, mean light minimum coincides with pulsation amplitude maximum. We find no statistically significant phase lag of the mean light extrema relative to pulsation amplitude maximum.

4 THE ROTATION PERIOD OF HD 99563

To infer the pulsational and magnetic geometry of HD 99563, its rotation period has to be known with certainty. However, at this point it is not clear whether the 7.95 μHz signal in the mean light variations and the frequency splitting within the pulsational signals correspond to the rotation period or to half the rotation period.

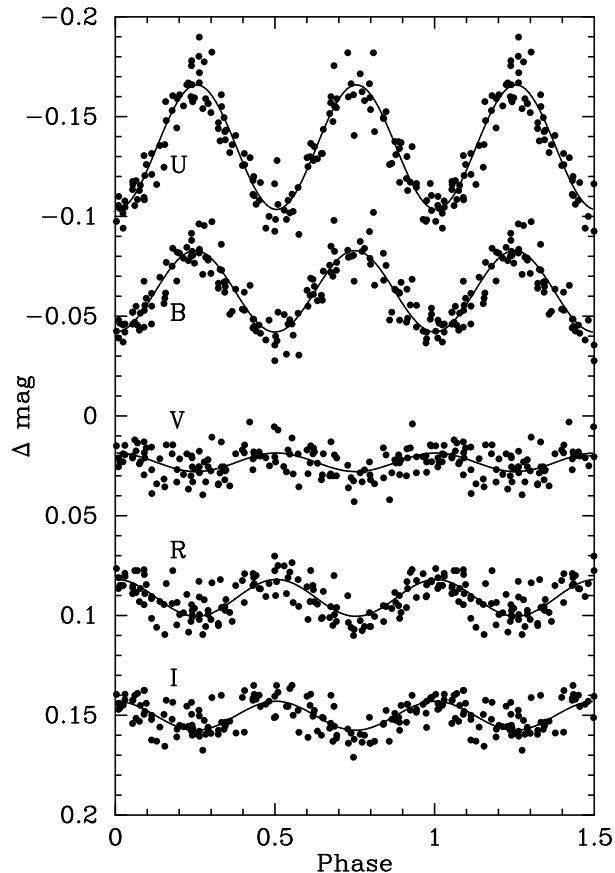


Figure 4. Mean UBVRI light variations of HD 99563 phased with a period of 2.91179 d. One and a half rotation cycles are shown. The solid line is the single-frequency fit from Table 3.

Since the magnetic field of the star also varies with aspect, we can invoke published magnetic field measurements for HD 99563 to resolve this ambiguity. Hubrig et al. (2004) measured a longitudinal magnetic field strength of -688 ± 145 G on HJD 2452494.479, whereas Kudryavtsev & Romanyuk (2005) measured $+580 \pm 100$ G on HJD 2453395.550.

Assuming a rotation frequency of 7.9498 ± 0.0002 μHz , the two measurements would have been taken 618.91 ± 0.02 rotational periods apart. Since these measurements would then have been taken at nearly the same rotation phase, but the magnetic field showed a reversal between these two measurements, such a rotation frequency can be ruled out. Using half this value (3.9749 ± 0.0001 μHz) implies that 309.455 ± 0.009 rotations have gone by, which is perfectly consistent with the magnetic field reversal between the two magnetic field observations and the absolute magnetic field strengths measured.

The correct value of the rotation period of HD 99563 is therefore close to 2.91 d. We show the corresponding phase diagram of the mean light variations of the star in Fig. 4.

5 FREQUENCY ANALYSIS (II)

Knowing that the rotation frequency of HD 99563 is near 3.975 μHz , we can now determine a final multifrequency solution for the pulsation data under the assumption of the

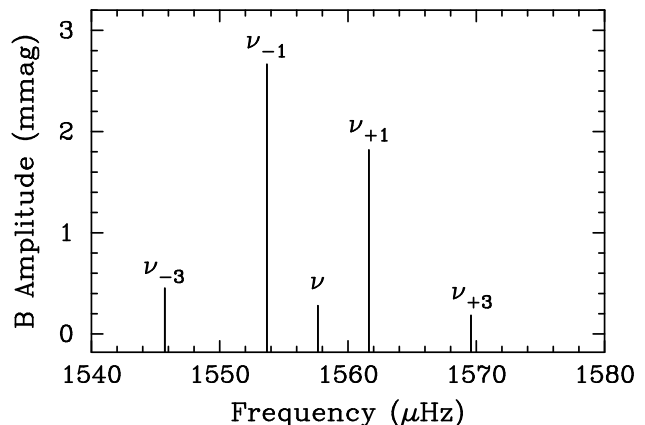


Figure 5. The frequency quintuplet detected in the light curves of HD 99563.

OPM. We first examine the variations in the frequency domain near 1550 μHz . The spacings within all the frequencies already detected in this range are consistent with this rotation frequency and thus belong to the same multiplet. We therefore searched for possible further multiplet components in the residual amplitude spectra that have $S/N > 3.5$. We indeed detected a peak near $f_5 = 1569.6$ μHz that is consistent with this splitting and has $S/N > 3.6$. Adding this signal to the four previously detected, we find a symmetrical series of peaks centred on $f_4 = 1557.6$ μHz , for which we show a schematic graphical representation in Fig. 5.

We can now derive a final frequency solution. To this end, we have started with the frequencies from the preliminary solution in Table 2, added f_5 and fitted these ten signals to the data. During this process, we fixed the signal frequencies to equal splitting, using a starting value of 3.9749 μHz , and we also demanded that harmonics occurred at exactly twice the “parent” frequency within Period98. With this procedure, we do not only determine final frequency values, but we also reduce the number of free parameters in the fit to a minimum. This should guarantee the most reliable and most stable frequency solution, and the rotation frequency will also be determined most accurately that way. The final result of our frequency analysis can be found in Table 4.

The splitting between the rotationally split components of the pulsation mode of HD 99563 is 3.9751 ± 0.0003 , which is the same as half the frequency of the mean light variations within the errors. Since we know that this splitting corresponds to the rotation frequency, we can fix the latter by averaging the two results into 3.9749 ± 0.0001 μHz , corresponding to a rotation period of 2.91179 ± 0.00007 d.

The referee has noted that relative phases of the first-order combination frequencies ($\phi(2\nu) - 2\phi(\nu) = 0.01 \pm 0.20$; $\phi(2\nu_{-1}) - 2\phi(\nu_{-1}) = -0.27 \pm 0.10$; $\phi(2\nu_{+1}) - 2\phi(\nu_{+1}) = 0.14 \pm 0.16$) are consistent with zero. This is an indication that the frequencies around 3115 μHz are indeed the first harmonics of the main pulsational signals near 1557 μHz .

6 DISCUSSION

The pulsational light variations of HD 99563 are due to a single pulsation mode at a frequency of 1557.6530 μHz . Due to the rotation of the star with a period of 2.91179 d, we

Table 4. Final multifrequency solution for our B filter data of the roAp star HD 99563, again with error estimates from Montgomery & O’Donoghue (1999; errors on frequencies and amplitudes are given in Table 2). Pulsation phases are with respect to pulsation amplitude maximum at HJD 2452031.29627.

ID	Frequency (μHz)	B Ampl. (mmag)	Phase (rad)
$\nu = f_4$	1557.6530	0.29	$+2.63 \pm 0.09$
$\nu_{-1} = f_4 - f_{\text{rot}}$	1553.6779	2.67	$+2.87 \pm 0.01$
$\nu_{+1} = f_4 + f_{\text{rot}}$	1561.6281	1.82	$+2.83 \pm 0.01$
$\nu_{-3} = f_4 - 3f_{\text{rot}}$	1545.7276	0.45	$+2.82 \pm 0.06$
$\nu_{+3} = f_4 + 3f_{\text{rot}}$	1569.5784	0.18	$+3.00 \pm 0.15$
2ν	3115.3060	0.32	-1.03 ± 0.08
$2\nu_{-1}$	3107.3557	0.25	-0.27 ± 0.10
$2\nu_{+1}$	3123.2562	0.17	-0.76 ± 0.16
$2\nu + f_{\text{rot}}$	3119.2811	0.15	-0.51 ± 0.18
$2\nu - 4f_{\text{rot}}$	3099.4055	0.13	$+0.55 \pm 0.21$
f_{rot}	3.9751		

see it at different aspect during the rotation cycle, which gives rise to an equally spaced frequency triplet. Two more multiplet components separated by three times the rotation frequency were also detected. These are an indication that the pulsation mode of HD 99563 is not a pure dipole, but is distorted by the effect of its magnetic field.

To examine the nature of this pulsation mode, we first need to know the inclination of the stellar rotation axis to the line of sight, which in turn requires an estimate of the stellar radius. Consequently, we first infer the star’s position in the HR Diagram.

HD 99563 is a visual binary with a secondary component 1.2 magnitudes fainter at a distance of $1.79''$ (Fabricius & Makarov 2000). Thus, photoelectric photometric observations of the system will include the secondary, which contributes 1/4 of the total light. (This also means that the amplitudes of the photometric variations we discussed here must be increased by one third to give intrinsic values.) The Tycho-2 photometry of the two components (Fabricius & Makarov 2000) transformed to the standard Johnson system by using the relations by Bessell (2000) gives: $V = 8.72$, $(B - V) = 0.20$ for HD 99563A and $V = 9.91$, $(B - V) = 0.285$ for HD 99563B. These values suggest that the two components could be physically associated.

The HIPPARCOS parallax of the system (ESA 1997) is 4.27 ± 2.02 mas. The galactic reddening law by Chen et al. (1998) then results in $A_v = 0.010 \pm 0.002$. Therefore one obtains $M_v = 1.9^{+0.8}_{-1.4}$ for HD 99563A and $M_v = 3.1^{+0.8}_{-1.4}$ for HD 99563B. Because of the large uncertainty of the HIPPARCOS parallax we can therefore not obtain a radius estimate of HD 99563A with sufficient accuracy, but we can, using also the $(B - V)$ estimated above, point out that HD 99563B is located inside the δ Scuti instability strip and may therefore also show pulsations. However, our check for low-frequency variability did not detect these.

To estimate the effective temperature of HD 99563 we can apply the calibration by Moon & Dworetzky (1985), who use the Strömgren H_β index as a temperature indicator. None of the other Strömgren indices is suitable for basic parameter determination of chemically peculiar A stars be-

cause of heavy line blanketing. The measured H_β value for HD 99563AB is 2.830 (Olsen & Perry 1984). With the V magnitude and $(B - V)$ colour differences given above, combined with the standard relation by Crawford (1979), we can determine $H_\beta = 2.844$ for HD 99563A and $H_\beta = 2.785$ for HD 99563B. The calibration by Moon & Dworetzky (1985) then gives $T_{\text{eff}} \sim 8050$ K for HD 99563A and $T_{\text{eff}} \sim 7400$ K for HD 99563B.

Elkin et al. (2005) performed a spectral analysis of HD 99563, which resulted in $T_{\text{eff}} = 7700$ K, $\log g = 4.2$ and $[M/H] = 0.5$ for the roAp star. We assume a generous $T_{\text{eff}} = 7900 \pm 300$ K and that HD 99563A is still on the main sequence, i.e. $\log g = 4.15 \pm 0.2$. Consequently, we estimate that $R = 1.9^{+0.6}_{-0.4} R_\odot$. The projected rotational velocity of HD 99563A is $28.5 \pm 1.1 \text{ km s}^{-1}$ (Elkin et al. 2005). Combined with the rotation period determined before, we then derive $i = 60^{+30}_{-19}$ degrees, a poor constraint. However, this also implies $R \geq 1.58 R_\odot$.

As a final attempt to derive the basic parameters of HD 99563A, we assumed that HD 99563B is a physical companion. Due to the wide separation of the two components, they would have evolved independently from each other. The goal now is to find two stellar models that have effective temperatures as determined above (for reasons of consistency, we take the photometric values for both stars), that have the same age, and the observed magnitude difference of HD 99563A and B.

We used the Warsaw-New Jersey stellar evolution code (e.g. see Pamyatnykh et al. 1998 for a description) to find such a pair of models. We computed stellar evolutionary tracks in the range between 1.5 to 2.2 M_\odot for $Z = 0.02$. We indeed found two models that satisfy the observational constraints. They have masses of 2.03 M_\odot (HD 99563A) and 1.585 M_\odot (HD 99563B), luminosities of 21.6 and 7.1 L_\odot respectively, and ages of 620 Myr. The model for HD 99563A has a radius of 2.38 R_\odot , which then implies $i = 43.6 \pm 2.1^\circ$. The internal accuracy of this method is high: changing the secondary mass by only $\pm 0.01 M_\odot$ already cannot reproduce the observations within the errors.

For the purpose of further discussion, we assume $i = 44^\circ$. We can now apply the OPM, which predicts

$$\frac{A_{+1} + A_{-1}}{A_0} = \tan i \tan \beta \quad (1)$$

(Shibahashi 1986), where the A_r ’s are the amplitudes of the r^{th} rotational sidelobes, i is the inclination of the stellar rotational axis to the line of sight and β is the magnetic obliquity. From the amplitudes in Table 4, we obtain $\tan i \tan \beta = 15.5 \pm 1.5$, hence $\beta = 86.4 \pm 0.3^\circ$. This is a perfectly reasonable result given the relative amplitudes in the central frequency triplet.

Within the framework of a regular perturbation treatment, Shibahashi & Takata (1993) derived an expected amplitude ratio

$$\frac{A_3 + A_{-3}}{A_2 + A_{-2}} = \frac{1}{6} \tan i \tan \beta, \quad (2)$$

which is consistent with our observational data that lead to a null results when searching for the ν_2 and ν_{-2} components of the stellar pulsation mode.

We further examine the distorted dipole mode of HD 99563 by applying the axisymmetric spherical harmonic de-

Table 5. Components of the spherical harmonic series description of the pulsation mode of HD 99563 for $i = 44^\circ$, $\beta = 86.4^\circ$.

ℓ	0	1	2	3
$A_{-3}^{(\ell)}$ [mmag]				0.450
$A_{-2}^{(\ell)}$ [mmag]			0.158	0.158
$A_{-1}^{(\ell)}$ [mmag]		3.405	0.037	-0.699
$A_0^{(\ell)}$ [mmag]	0.237	0.376	-0.093	0.042
$A_{+1}^{(\ell)}$ [mmag]		2.372	0.028	-0.524
$A_{+2}^{(\ell)}$ [mmag]			0.088	0.088
$A_{+3}^{(\ell)}$ [mmag]				0.180
$\phi^{(\ell)}$ [rad]	0.024	2.859	-0.322	2.820
$C_{n\ell}\Omega/K^{mag}$		0.107	0.020	0.010

Table 6. Comparison of the observed amplitudes and phases of the distorted dipole pulsation mode of HD 99563 and our spherical harmonic fit.

ID	A_{obs}	A_{calc}	ϕ_{obs}	ϕ_{calc}
ν	0.29 ± 0.03	0.29	$+2.63 \pm 0.09$	+2.63
ν_{-1}	2.67 ± 0.03	2.67	$+2.87 \pm 0.01$	+2.87
ν_{+1}	1.82 ± 0.03	1.82	$+2.83 \pm 0.01$	+2.87
ν_{-2}	0.00 (assumed)	0.00	-----	n/a
ν_{+2}	0.00 (assumed)	0.00	-----	n/a
ν_{-3}	0.45 ± 0.03	0.45	$+2.82 \pm 0.06$	+2.82
ν_{+3}	0.18 ± 0.03	0.18	$+3.00 \pm 0.15$	+2.82

composition method by Kurtz (1992) which is based on the theory by Shibahashi & Takata (1993), to our data. This technique breaks the magnetically distorted mode up into its pure $\ell = 0, 1, 2, \dots$ spherical harmonic components and consequently allows one to infer the shape of the mode. We applied the method to our frequency solution (Table 4), assuming zero amplitude for the unobserved ν_{-2}, ν_{+2} components of the mode. The result is given in Tables 5 and 6.

From the values in Table 5 it can be seen that the mode of HD 99563 is dominated by the dipole component, which is reasonable as the magnetic fields in Ap stars are predominantly dipoles. The contribution of the $\ell = 0$ and $\ell = 2$ terms to the mode are fairly small, but the $\ell = 3$ component does have some influence. Table 6 shows that the observations are quite well reproduced by our fit. It would be interesting to see whether the theory by Saio & Gautschi (2004) is capable of reproducing our results.

We can now check how well our model reproduces the observed pulsational amplitudes and phases over the stellar rotation cycle. To this end, we subdivided the time series into pieces some 4–5 pulsation cycles long and determined the amplitudes and phases for the $1557.653 \mu\text{Hz}$ variation within these subsets. The spherical harmonic decomposition method by Kurtz (1992) yields a fit to the amplitude/phase behaviour over the rotation cycle, and we show it together with the data in Fig. 6.

We can see that both magnetic (pulsation) poles are actually in view for approximately the same amount of time; the relative fractions are 53 and 47 per cent. This is also the reason why it was so difficult to determine the rotation

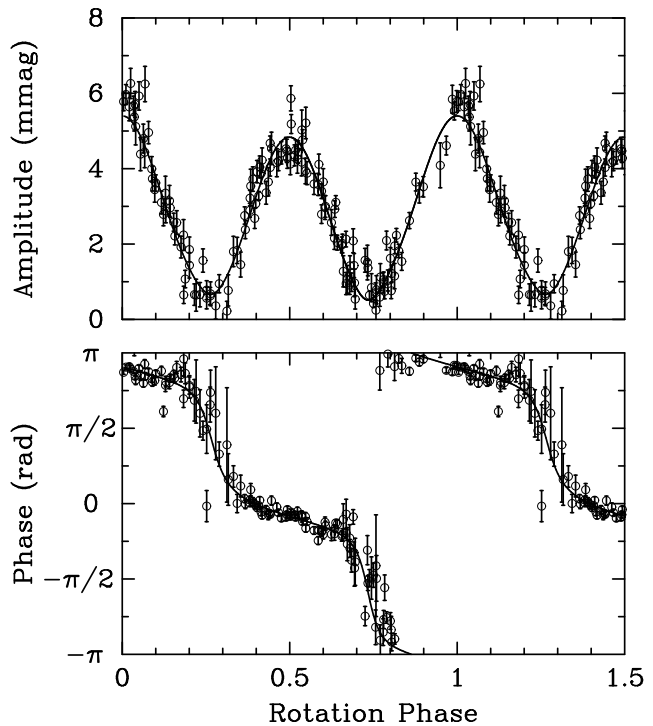


Figure 6. Pulsational amplitudes and phases relative to a rotation period of 2.91179 d. Phase zero corresponds to pulsation amplitude maximum, and one and a half rotation cycles are shown. The line is a fit computed with Kurtz' (1992) spherical harmonic decomposition method.

period of the star; the pulsations as well as the mean light variations are almost symmetrical along the rotation period.

The fitted curves reproduce the observations fairly well, with one exception: the pulsation amplitude is overestimated for the pole that is for a shorter time in the line of sight, whereas the amplitude is underestimated for the other pole. The harmonic frequencies cannot be made responsible for this, because they do not affect the first-order amplitudes analysed here. Consequently, we believe that the poor fits near the pulsation amplitude maxima could be due to presently undetected additional multiplet components of the pulsation mode; the amount of over- and under-fitting can be fully explained with the noise level in our residual amplitude spectrum.

7 CONCLUSIONS

Our photometric multisite observations of the roAp star HD 99563 resulted in the detection of a frequency quintuplet that is due to a single distorted dipole pulsation mode. The splitting within this frequency quintuplet together with our mean light observations and published magnetic measurements allowed us to determine the stellar rotation period as 2.91179 ± 0.00007 d. Within the errors, the mean light extrema occur in phase with pulsation amplitude maximum, suggesting that the abundance spots on HD 99563 should be fairly concentric around its magnetic poles.

To our knowledge, HD 99563 is only the fourth roAp star where both magnetic poles become visible throughout a rotation cycle (the others are HR 3831, e.g., see Kurtz et

al. (1993), HD 6532, e.g., Kurtz et al. (1996), and HD 80316 e.g., Kurtz et al. (1997)), and only the third whose pulsational mode distortion has been quantified. In this context it is interesting to note that the observational features of HD 99563 are in many aspects similar to another roAp star, the well-studied HR 3831 (e.g., Kurtz et al. 1993, Kochukhov 2004): their geometrical orientations, rotation period and effective temperatures are alike. Only the pulsation period of HD 99563 is some 10 per cent shorter, and the phases its first-order combination frequencies are more consistent with them being harmonics. It would thus be very interesting to compare these two objects in detail.

This would however require more in-depth studies of HD 99563. Its basic parameters are still poorly known; the radius we inferred is based on the assumption that the visual companion is physical, which needs to be checked. If HD 99563 A and B were a physical pair, then the separation of the components is too wide for motion around a common centre of mass to be determined in a reasonable period of time. However, common proper motion may be detectable within a few years.

The most efficient way to pin down the radius of the roAp star would perhaps come from a combination of magnetic and polarisation measurements (Landolfi et al. 1997). With that, the inclination i and the magnetic obliquity β can be constrained, and given the accurate rotation period and $v \sin i$ already available, a fairly accurate radius could be obtained.

There are several other possibilities that make HD 99563 interesting for future observations. As already argued by Elkin et al. (2005), the star is a very attractive target for pulsational radial velocity measurements. Given the high amplitude of the mean light variations of the star and its favourable geometry, Doppler Imaging of its surface should also be within reach. Finally, we have evidence that we have not yet deciphered the full pulsational content of the star's light curves. Another multi-site campaign, aiming at obtaining > 200 h of observations on 1-metre-class telescopes would therefore also be justifiable. As we pointed out, HD 99563B is located within the δ Scuti instability strip and should therefore also be tested for pulsations, with more suitable means than ours.

ACKNOWLEDGEMENTS

The Austrian Fonds zur Förderung der wissenschaftlichen Forschung partially supported this work under grants S7303-AST and S7304-AST. We are grateful to Don Kurtz for supplying results prior to publication, for helpful discussions and for comments on a draft version of this paper. We also thank Hiromoto Shibahashi for his accurate referee's report.

REFERENCES

- Bessell M. S., 2000, *PASP* 112, 961
 Breger M., 1979, *PASP* 91, 5
 Breger M., et al., 1999, *A&A* 349, 225
 Chen B., Vergely J.L., Valette B., Carraro G., 1998, *A&A* 336, 137
 Crawford D. L., 1979, *AJ* 84, 1858
 Cunha M. S., Gough D. O., 2000, *MNRAS* 319, 1020
 Dorokhova T. N., Dorokhov N. I., 1998, in *Proceedings of the 26th meeting of the European Working Group on CP stars*, Contributions of the Astronomical Observatory Skalnaté Pleso, p. 338
 Elkin V. G., Kurtz D. W., Mathys G., 2005, *MNRAS*, in press
 ESA, 1997, *The Hipparcos and Tycho catalogues*, ESA SP-1200
 Fabricius C., Makarov V. V., 2000, *A&A* 356, 141
 Handler G., Paunzen E., 1999, *A&AS* 135, 57
 Handler G., et al., 2000, *MNRAS* 318, 511
 Handler G., et al., 2002, *MNRAS* 330, 153
 Hubrig S., Szeifert T., Schöller M., Mathys G., Kurtz D. W., 2004, *A&A* 415, 685
 Jerzykiewicz M., et al., 2005, *MNRAS* 360, 619
 Kaye A. B., Handler G., Krisciunas K., Poretti E., Zerbi F. M., 1999, *PASP* 111, 840
 Kochukhov O., 2004, *ApJ* 615, L149
 Kochukhov O., Drake N. A., Piskunov N., de la Reza R., 2004, *A&A* 424, 935
 Kudryavtsev D. O., Romanyuk I. I., 2005, private communication to Elkin et al. (2005)
 Kurtz D. W., 1982, *MNRAS* 200, 807
 Kurtz D. W., 1992, *MNRAS* 259, 701
 Kurtz D. W., Martinez P., 2000, *Baltic Astronomy* 9, 253
 Kurtz D. W., Elkin V. G., Mathys G., 2003, *MNRAS* 343, L5
 Kurtz D. W., Kanaan A., Martinez P., 1993, *MNRAS* 260, 343
 Kurtz D. W., Martinez P., Koen C., Sullivan D. J., 1996, *MNRAS* 281, 883
 Kurtz D. W., Martinez P., Tripe P., Hanbury A. G., 1997, *MNRAS* 289, 645
 Landolfi M., Bagnulo S., Landi degl'Innocenti M., Landi degl'Innocenti E., Leroy J. L., 1997, *A&A* 322, 197
 Lueftinger T., Kuschnig R., Piskunov N. E., Weiss W. W., 2003, *A&A* 406, 1033
 Martinez P., et al., 2002, *Mon. Not. Astron. Soc. South Africa* 61, 102
 Matthews J. M., Kurtz D. W., Martinez P., 1999, *ApJ* 511, 422
 Montgomery M. H., O'Donoghue D., 1999, *Delta Scuti Star Newsletter* 13, 28 (University of Vienna)
 Moon T. T., Dworetzky M. M., 1985, *MNRAS* 217, 305
 Olsen E. H., Perry C. L., 1984, *ApJS* 56, 229
 Pamyatnykh A. A., Dziembowski W. A., Handler G., Pikall H., 1998, *A&A* 333, 141
 Ryabchikova T., Piskunov N., Kochukhov O., Tsymbal V., Mittermayer P., Weiss W. W., 2002, *A&A* 384, 545
 Saio H., Gautschi A., 2004, *MNRAS* 350, 485
 Shibahashi H., 1986, in *Hydrodynamic and Magnetohydrodynamic Problems in the Sun and Stars*, ed. Y. Osaki, University of Tokyo, p. 195
 Shibahashi H., Takata M., 1993, *PASJ* 45, 617
 Sperl M., 1998, Master's thesis, University of Vienna
 Takata M., Shibahashi H., 1995, *PASJ* 47, 219